Seasonal Controls on Nearshore Hypoxia in a Small Coastal Embayment

A Senior Thesis
presented to
the Faculty of the Physics Department
California Polytechnic State University – San Luis Obispo

In Partial Fulfillment
of the Requirements for the Degree
Bachelor of Sciences
in
Marine Science

by

Stephen Alexander Huie

March 2021

Approval Page

Title: Seasonal Controls on Nearshore Hypoxia in a Small Coastal Embayment

Author: Stephen Huie

Date Submitted: 3/18/2021

Senior Thesis Advisor: Dr. Ryan Walter

_____

Signature

_____

Date

1 Introduction

Dissolved oxygen (DO) is an important biogeochemical factor that strongly influences nearshore coastal ecosystems. When DO concentrations fall below a certain threshold, the water is considered hypoxic (Vaquer-Sunyer and Duarte, 2008). When macroorganisms encounter these hypoxic environments, they are physiologically stressed, and in some cases, low DO levels can lead to mass mortalities of ecologically and economically important species (Grantham et al, 2004). Coastal hypoxia has drawn significant attention in recent years due to increases in the frequency and duration of these hypoxic events (Chan et al. 2008). Due to this, as well as climate-change-driven warming and the subsequent deoxygenation of the world's oceans, it is important to understand nearshore drivers of DO variability (Du et al. 2018).

DO variability is controlled by various physical and biological processes that vary on a wide range of timescales, including seasonally and synoptically (i.e., event-scale). The dominant physical processes that influence hypoxia along Eastern Boundary Upwelling Systems (EBUS) are wind-driven coastal upwelling and density stratification. Coastal upwelling results in the advection of cold, nutrient-rich, low DO waters from the deep offshore into the nearshore (Adams et al. 2013). The intensity of the upwelling is dependent on the magnitude of winds blowing equatorward and parallel to the coastline (cf. Chavez and Messié, 2009). Stronger and longer-duration upwelling wind events can lead to the lifting of isopycnals and intrusions of low DO conditions in the nearshore, often approaching the hypoxic limit (Booth et al. 2012; Walter et al. 2014; Boehm et al. 2015 and references therein). In addition to upwelling, strong vertical density stratification can lead to a vertical mixing barrier between the surface and bottom waters. Thus, during periods of strong stratification, surface waters higher in DO due to air-sea gas exchange are confined to surface layers. This barrier to vertical mixing is particularly amplified

when coupled with high rates of respiration in near-bottom waters that drive down DO levels (Bailey, 1991). Consumption of DO occurs when organic matter in the water column and sediments is degraded by microbial communities and grazers, particularly following large phytoplankton blooms (Connolly, 2010; Pitcher and Probyn, 2011). Understanding the concomitant role of these physical and biological processes is critical to better understand the development of nearshore hypoxia.

Furthermore, it is also important to understand how seasonal changes in these processes influence DO variability and hypoxia risk. In eastern boundary currents, upwelling seasonality helps shape the physical and biological environment (e.g., Garcia -Reyes and Largier, 2012; Walter et al. 2018). During the spring and early summer, peak upwelling occurs and the nearshore is characterized by minimal vertical stratification, the influx of cold upwelled waters at the near bottom, and peaks in chlorophyll concentrations driven by the addition of nutrients into the photic zone and subsequent growth of phytoplankton (Pennington and Chavez, 2000; Walter et al. 2018). The nutrient-rich waters during this time of the year typically support fast-growing and long, chain-forming diatoms (Barth et al. 2020). As the summer progresses and the upwelling wind begins to relax, the nearshore develops significant vertical stratification, conditions that tend to favor dinoflagellate blooms (Walter et al. 2018; Barth et al. 2020). Seasonal changes in phytoplankton community structure are influenced by physical processes, and both work in tandem to alter DO variability.

Along with seasonal influences on DO variability that act over broader spatial scales, coastline orientation and complex topography can lead to extensive variability in local processes and upwelling and hence hypoxia risk (see recent review by Largier, 2020). In particular, embayments in upwelling systems are ubiquitous (i.e., “upwelling bays”), and these embayments

can amplify/reduce the influence of upwelling processes (Largier, 2020). In many upwelling bays, upstream headlands block regional upwelling winds, leading to increased residence times and warming inside the bay ("upwelling shadow") relative to the colder upwelling waters outside the bay (e.g., Woodson et al. 2009; Walter et al. 2018). The retention and stratification that develops in upwelling shadows can lead to conditions favorable for dense phytoplankton blooms (particularly dinoflagellates) and have appropriately been called local bloom incubators (Ryan et al. 2008; Barth et al. 2020; Largier 2020;). Thus, upwelling bays may be particularly prone to hypoxia during periods of strong stratification when decomposition and respiration below the thermocline draw down DO levels.

In this study, we assess the role of a small upwelling bay and shadow system (San Luis Obispo Bay in Central California) on nearshore DO variability and hypoxia risk. We collected near-bottom and near-surface DO at three nearshore sites (inside and outside the bay) over the full upwelling season, in conjunction with periodic offshore profiles, to evaluate seasonal and spatial drivers of DO variability In addition to physical processes, we also investigate the role of phytoplankton community composition on DO dynamics to describe the seasonal controls on DO variability in this system. Dynamical and ecological ramifications of the findings are discussed.

2 Data and Methods

2.1 Site Description

San Luis Obispo (SLO) Bay is a semi-enclosed embayment located along the Central California Coast located between Point San Luis to the north and Point Sal to the south (Figure 1a). SLO Bay is home to a commercial fishing port, kelp forests that support large biodiversity, and the California Polytechnic (Cal Poly) State University Pier. SLO bay is classified as a small bay, with length and width scales much less than 20 km (Largier, 2020). The very northern

portion of the bay is ~ 3 km wide and has a shallow average depth of ~ 10 m (Figure 1b) SLO Bay is characterized by an "upwelling shadow" which is a region shielded from upwelling favorable winds by a landmass (Walter et al, 2018).

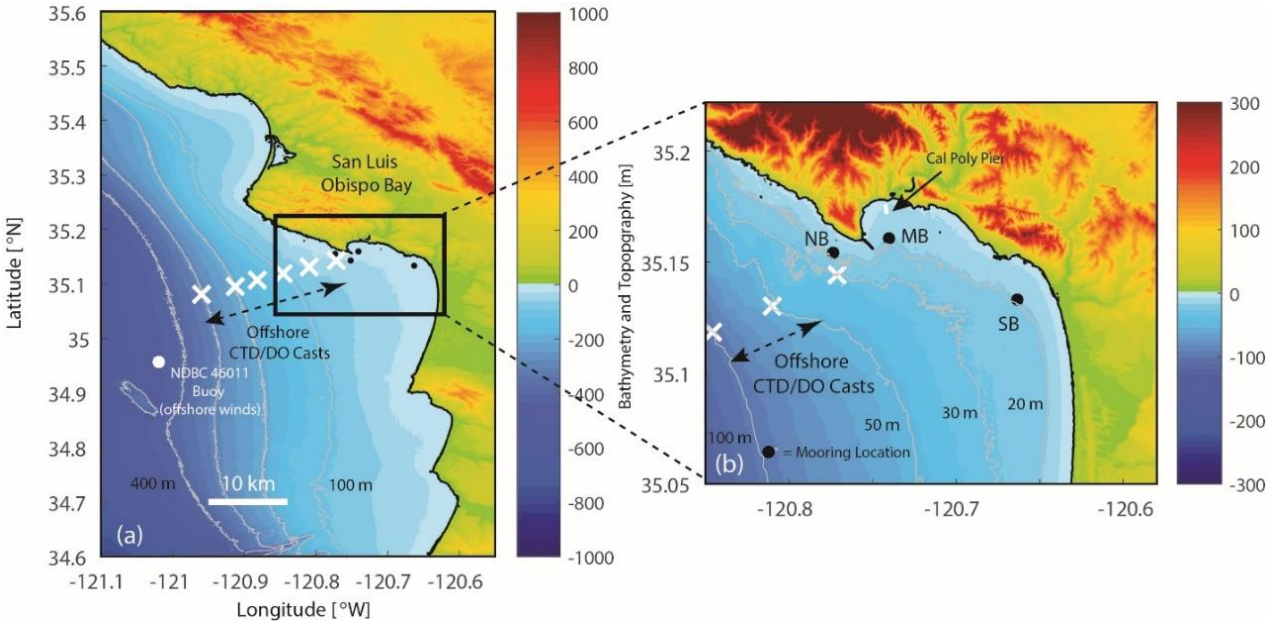

Figure 1: Topography and bathymetry of the San Luis Obispo Bay study region in Central California. (Left) Zoomed out view of the region highlighting the locations of the offshore CTD/DO casts (white 'X') and the regional buoy used to measure upwelling winds. (Right) Zoomed in view of San Luis Obispo Bay highlighting mooring locations (black dots) in the North Bay (NB), Middle Bay (MB), and South Bay (SB), as well as the location of the Cal Poly Pier (thick white line).

2.2 Experimental Set Up

Three near-shore oceanographic moorings were deployed in SLO Bay at the start of the upwelling season in March 2017 and recovered during the upwelling relaxation season in August 2017. All three moorings were located along the 18 m isobath at distinct geographic locations inside and outside the bay (Figure 1b). These moorings were all equipped with thermistors (RBR Solo T, 5 s sampling period, 2 m vertical spacing), near bottom conductivity-temperature-depth (CTD) sensors with optical dissolved oxygen (DO) sensors [Sea-Bird Scientific MicroCAT 37 SMP-ODO, 10 min sampling period, 2 meters above the bed (mab)], and near-surface DO

sensors (PME MiniDOT, 1 min sampling period, 15 mab). Optical DO sensors were calibrated prior to the deployment by the manufacturer. They also contained biofouling prevention measures (pumped system with anti-foulant devices on the Sea-Bird instruments and copper mesh/wire guard on the PME instruments) and were cleaned approximately monthly by divers

In addition to the moorings, a profiling water quality package at the Cal Poly Pier supported by the Central and Northern California Ocean Observing System (CeNCOOS) measured vertical profiles of temperature, salinity, and chlorophyll fluorescence (cf. Walter et al. 2018). Additionally, weekly surface phytoplankton abundance and community data were obtained from the Harmful Algal Blooms sampling station at the Cal Poly Pier supported by the Southern California Coastal Ocean Observing System (SCCOOS). Regional upwelling favorable winds were calculated by rotating winds from offshore NDBC buoy 46011 (Figure 1a) to be parallel to the coast and equatorward (150° from true north, cf. Walter et al. 2018).

The nearshore measurements were supplemented by offshore CTD/DO vertical profiles obtained along repeated cross-shore transects going from 30 m to 300 m depth (see Figure 1). These occurred approximately monthly from March 2017 to August 2017 onboard Cal Poly's R/V TL Richards using a Sea-Bird Scientific 19+ profiling CTD and an electrochemical DO sensor (SeaBird 43) to obtain vertical profiles of temperature, salinity, and DO. These hydrographic transects, along with moored measurements, were used to track the seasonal evolution and cross-shelf distribution of water mass properties and DO under a variety of wind-driven upwelling and physical forcing regimes. The casts were used to assess source water variability and provide a link between offshore and nearshore water masses.

2.3 Data Processing

To assess the role of lower-frequency physical process on DO variability, hourly averaged data were low-passed filtered using a 33 hr low-pass filter to remove higher frequency fluctuations possibly driven by tides, local diurnal wind forcing, upwelling fronts, and internal waves (cf. Walter et al. 2017). The role of higher-frequency processes will be investigated in a future study.

3 Results

3.1 General Observations

Upwelling winds were stronger, but more variable during the spring and decreased in magnitude and variability during the late summer (Figure 2a). Nearshore surface and bottom temperatures at all sites progressively warmed from spring to summer, with vertical differences (i.e., temperature stratification) increasing substantially in the summer (Figures 2b and 2c). Surface waters displayed more temperature variance compared to bottom waters. Bottom water temperatures were generally consistent across the three nearshore sites, while at the surface, the outside bay site (NB) was consistently colder than the inside bay sites (MB and SB), particularly in the late summer. Dissolved oxygen (DO) also displayed less variance near the bottom, with levels dropping below the hypoxic threshold of 4.6 mg/L (Vaquer-Sunyer and Duarte, 2008), during both the late spring and late summer (Figures 2d and 2e). Similar to temperature, surface DO was much higher and more variable compared to the bottom, with surface DO outside the bay (NB) typically displaying lower DO levels compared to those inside the bay (MB and SB). Depth-integrated chlorophyll from the Cal Poly Pier showed synoptic-scale (i.e., event-scale) variability in chlorophyll levels during late spring and again in late summer (Figure 2f). The

phytoplankton community was primarily composed of diatoms in the spring and early summer, transitioning to dinoflagellates in the late summer (Figure 2g).

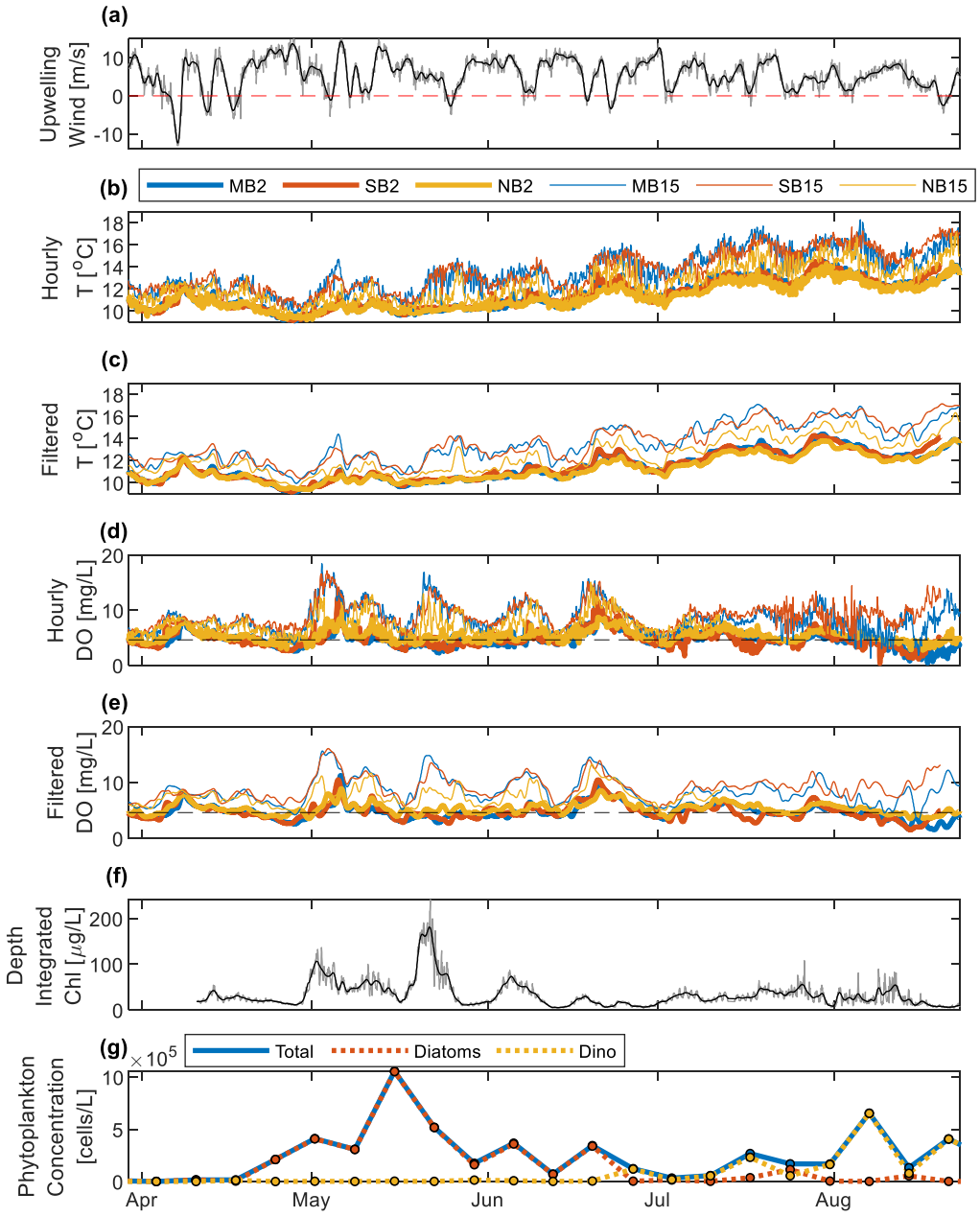

Figure 2: Time series from late March to late August. (a) Upwelling favorable winds, with the hourly (grey) and low-pass filtered (black) data. (b) Hourly temperature, (c) low-pass filtered temperature, (d) hourly dissolved oxygen, and (e) low-pass filtered dissolved oxygen at each mooring (MB – blue, SB – red, NB – orange). The thick lines in the panels b-e correspond to the near-bottom (2 mab) measurements, while the thin lines denote the near-surface (15 mab). The dashed line in panels (d) and (e) represents the hypoxic threshold of 4.6 mg/L (Vaquer-Sunyer and Duarte, 2008). (f) Depth-integrated chlorophyll measured from the Cal Poly Pier profiler (gray) and the low-pass filtered quantity (black). (g) Phytoplankton concentration from the Cal Poly Pier HABs sampling program.

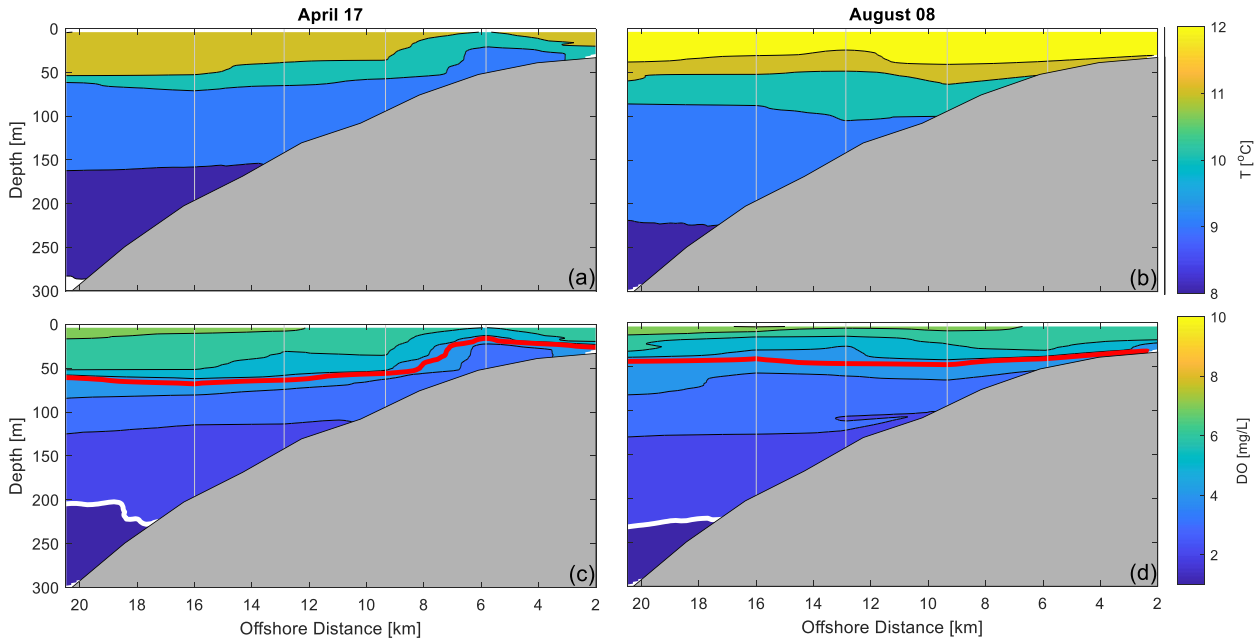

Figure 3: Cross-shelf depth contours from the April 17 (left) and August 8 (right) cruises for temperature (a and b) and dissolved oxygen (c and d). The red line in (c) and (d) denotes the hypoxic threshold of 4.6 mg/L, while the white line denotes the anoxic threshold of 2.0 mg/L (CITE). Vertical gray lines show the location of CTD/DO casts used for the contouring.

3.2 Offshore Observations

Figure 3 shows representative cross-shelf depth contours of temperature and oxygen from the spring and late summer. In the spring, isotherms and lines of constant oxygen slope upwards and shoal towards the surface, with low DO hypoxic bottom waters observed on the innermost portion of the shelf within a few kilometers of the shoreline (Figure 3a and 3c). This example highlights the advection of low DO subthermocline waters into shallow waters. Later in the summer, isotherms and lines of constant oxygen are flatter, with increased temperature stratification observed in the upper portion of the water column and less low DO water close to shore (Figure 3b and 3d).

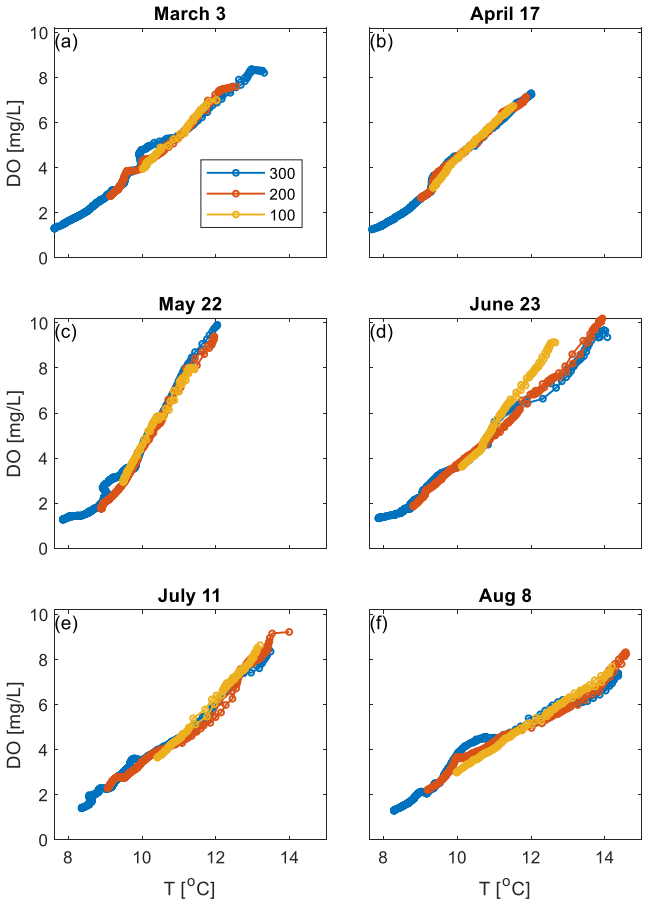

Figure 4: Temperature-DO relationship at the 300 m (blue), 200 m (red), and 100 m (orange) depth locations for all offshore cruises.

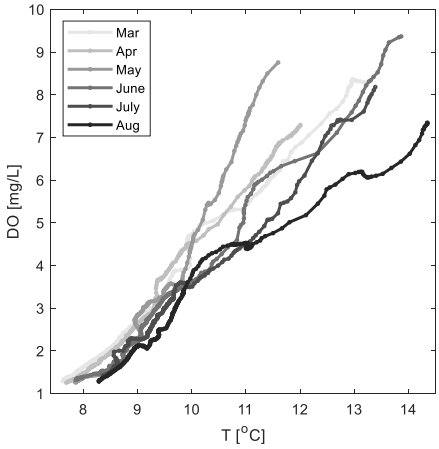

Figure 5: Temperature-DO relationship at the 300 m depth location for all offshore cruises. Color assigned based on the month of the cruise.

Examination of the temperature-DO (T-DO) relationship from the 100, 200, and 300 m vertical profiles for each respective sampling day reveals a consistent relationship at all profiling depths (Figure 4). Moreover, the low T-DO region of the parameter site is consistent across all sampling dates, whereas the high T-DO region is more variable and displays a slight seasonality tending towards higher T and lower DO later in the summer (Figure 5).

3.3 Nearshore Observations

The offshore T-DO relationships are used in conjunction with the nearshore T-DO data to assess possible mechanisms that drive DO variability in the nearshore. The near-bottom, nearshore T-DO data across all three sites line up with the offshore T-DO data in the low T-DO region of the parameter space. In the high T-DO portion of the parameter space, there are significant nearshore deviations (lower DO for a given T), particularly inside the bay (MB and SB). In general, sites inside the bay (MB and SB) showed a greater number of hypoxic events and lower DO concentrations relative to outside the bay (NB).

Closer examination of the hypoxic events reveals two distinct regimes in the T-DO parameter space. In the low T-DO hypoxic regime when the nearshore and offshore relationships align, there are the strongest upwelling winds (Figure 6a-c), with minimal vertical stratification (Figure 6d-f), and minimal vertical DO differences (Figure 6g-i). This suggests that these hypoxic events are driven by the advection of offshore waters into the nearshore during the peak upwelling periods in the spring (see also Figure 3c). In the other hypoxic regime at higher temperatures, there are additional near-bottom nearshore hypoxic events that do not align with the offshore T-DO relationship, with the nearshore DO concentrations significantly lower relative to the offshore waters at the same temperature. These nearshore deviations from the

offshore T-DO relationship are also significantly more pronounced inside the bay (MB and SB) compared to outside the bay (NB). These events are characterized by weak to moderate upwelling (late summer) (Figure 6a-c), the strongest vertical stratification (Figure 6d-f), and the largest vertical DO differences (Figure 6g-i). At NB, there were only minimal nearshore differences from the offshore T-DO relationship and vertical temperature stratification was minimal at higher temperatures (Figure 6g-i).

Unlike the physical parameters (upwelling strength and vertical stratification), there were minimal trends between depth-integrated-chlorophyll inside the bay (no chlorophyll data available outside the bay) and the offshore and near-bottom nearshore T-DO relationship at all sites. The highest depth-integrated chlorophyll-values inside the bay do tend to occur in the low T-DO regime (although not significantly below the hypoxic threshold), with moderate values in the higher temperature regime (Figure 6j-l).

Compared to the near-bottom nearshore T-DO data, the near-surface data displayed significantly more variability, but with DO concentrations significantly higher than near-bottom values and staying above the hypoxic threshold almost exclusively (Figure 7). The nearshore data outside the bay (NB) show more correspondence with the data inside the bay (MB and SB), with the inside bay nearshore data showing larger DO concentrations for a given temperature, particularly at higher temperatures. Similar to the near-bottom, the near-surface T-DO relationship aligns with the offshore T-DO relationship during periods of strong upwelling winds; however, DO stays above the hypoxic threshold (Figure 7a-c). Generally, the high T-DO portion of the parameter space displayed the largest vertical stratification (Figure 7d-f) and vertical DO differences (Figure 7g-i) (NB showed minimal vertical differences in temperature and DO) but does not strongly deviate from the general offshore T-DO relationship. The largest

DO values were observed when the depth-integrated chlorophyll inside the bay was also largest, suggesting local production via photosynthesis (Figure 7j-i). Outside the bay at NB (no chlorophyll data available), DO concentrations were not as high during these events.

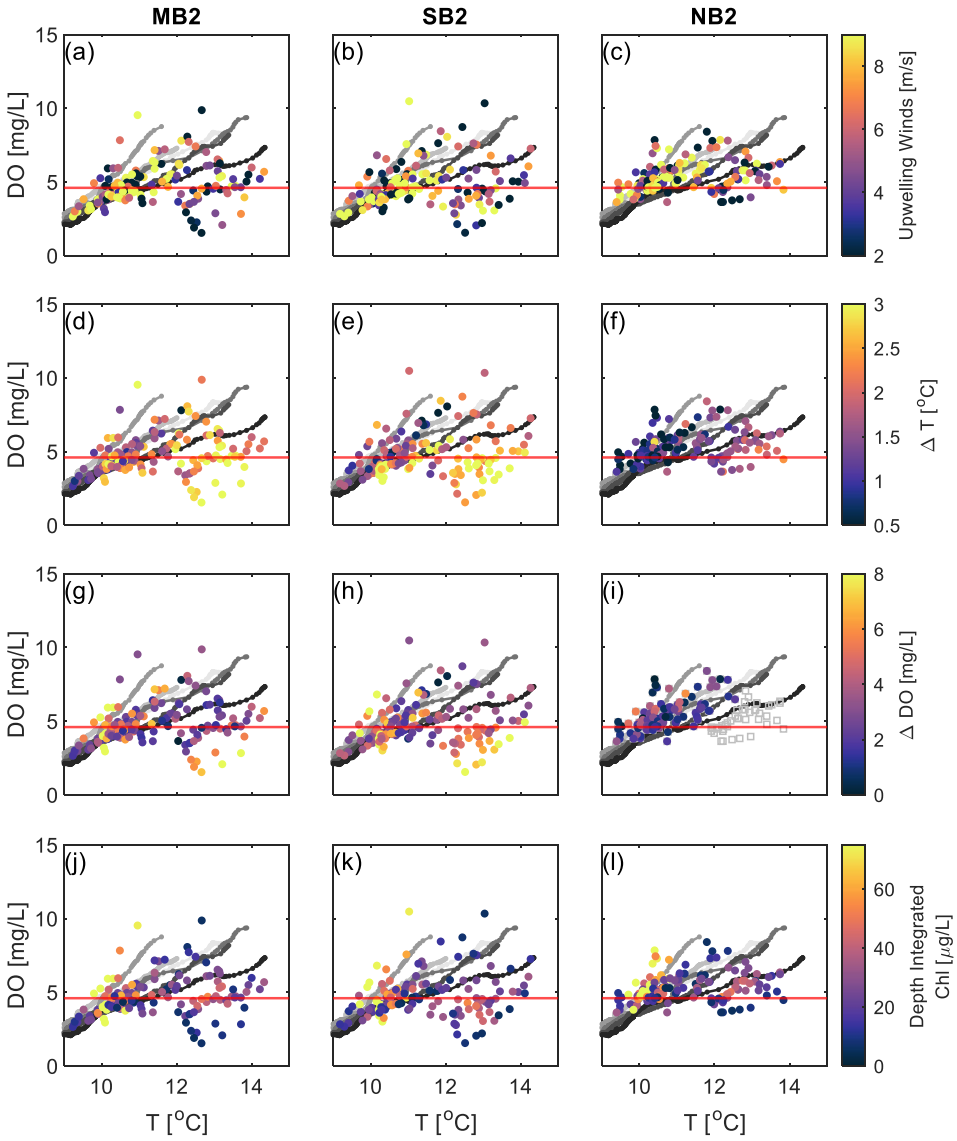

Figure 6: Near-bottom (2 mab) temperature-DO relationship from MB (left column), SB (middle column), and NB (right column). Hourly data are low-pass filtered and then downsampled (one point every 24 hrs) for visualization. The colors on each plot represent the offshore upwelling favorable winds (a-c), top to bottom temperature difference at the respective site (d-f), top to bottom DO difference at the respective site (g-i), and depth-integrated chlorophyll at the Cal Poly Pier. Also shown in each plot in small grayscale points are the offshore T-DO relationship from 300 m, with the earliest cruise in the lightest gray and the latest cruise in black. The hypoxic threshold of 4.6 mg/L is shown as a horizontal red line in all plots. In panel (i), gray squares are shown when near-surface DO data were not available.

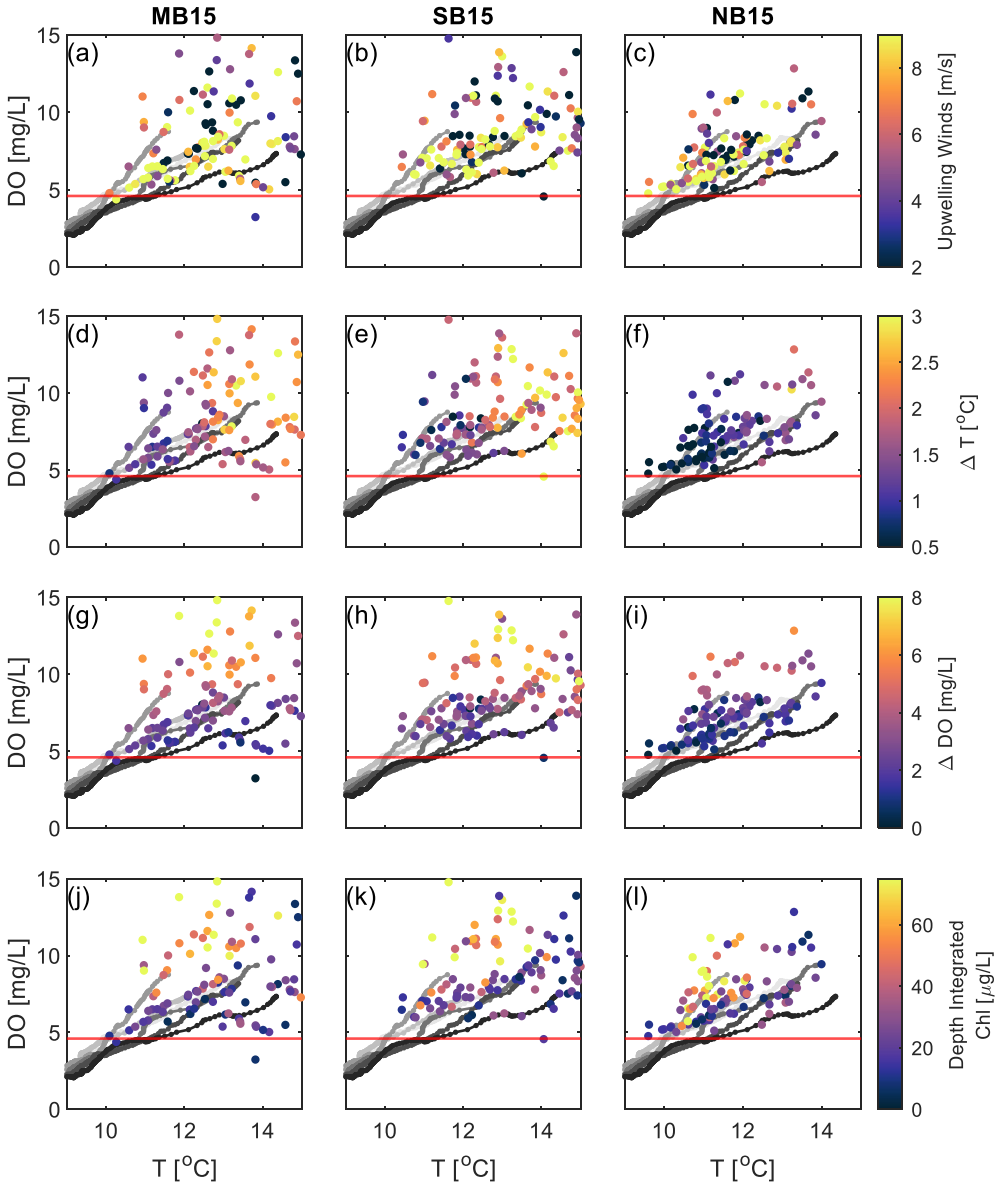

Figure 7: Same as Figure 6 but for the near-surface (15 mab).

3.4 Spatial Comparisons in the Nearshore

To further investigate spatial differences in DO between the nearshore sites, we compared near-bottom and near-surface DO between MB and SB (Figure 8) and MB and NB (Figure 9). Generally, MB and SB (both inside the bay) show good agreement between both the

near-bottom and near-surface DO across different upwelling conditions (Figure 8a and 8b). Also, horizontal temperature differences between the locations remained relatively low with small near-surface increases in DO at SB at low DO values when SB was slightly warmer (Figure 8d).

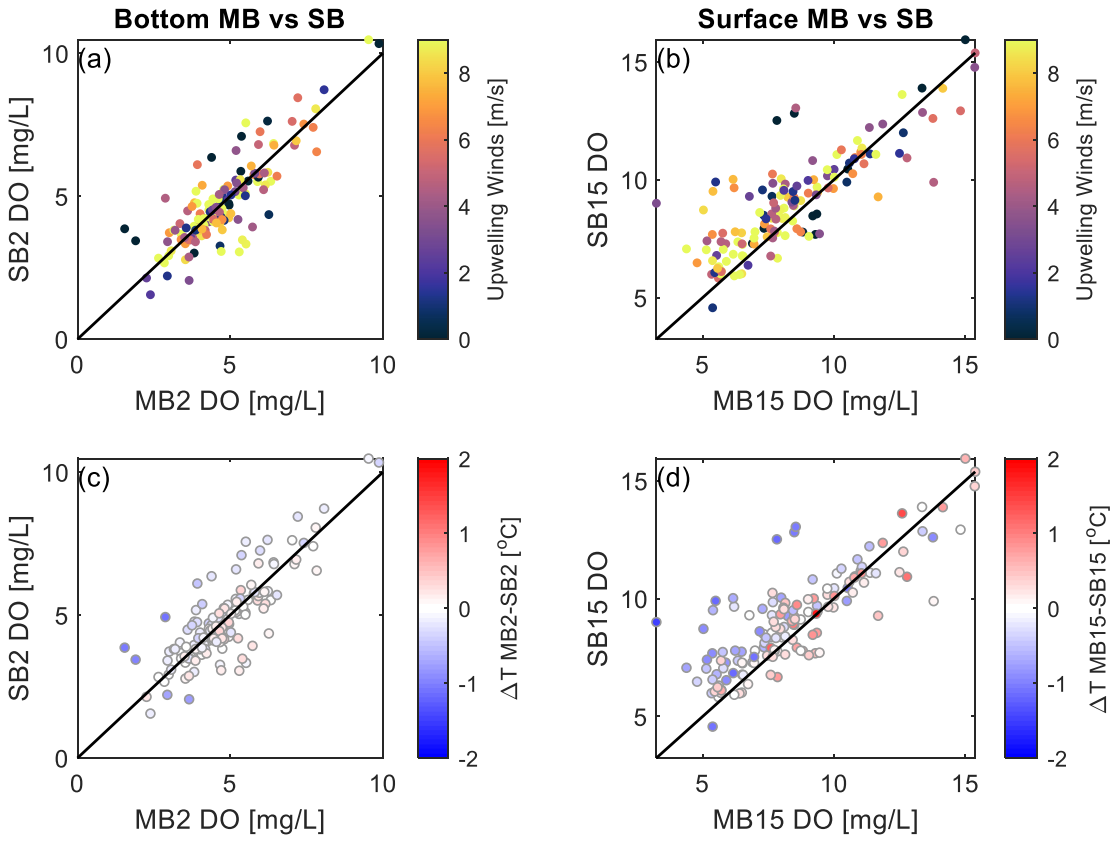

Figure 8: DO scatterplots between MB and SB for the near-bottom (a and c) and near-surface (b and d) locations. In (a) and (b), points are colored based on the upwelling favorable winds. In (c) and (d) the points are colored based on the temperature difference between MB and SB at the respective vertical location. All hourly data shown are low-pass filtered and then downsampled (one point every 24 hr) for visualization. A black one-to-one line is also shown.

Comparing MB (inside bay) and NB (outside bay), there are more significant differences in DO (Figure 9). At the bottom, there is a slight trend that NB has higher DO compared to MB (Figure 9a and 9c). At the surface, MB has much higher DO compared to NB, particularly in the high DO range, with MB having consistently warmer near-surface waters compared to NB.

To further investigate spatial gradients in temperature between MB and NB, we computed full water-column temperature differences between MB and NB over the entire time series (Figure 10). Significant temperature differences of more than 2 ºC are consistently present, particularly during the late summer and early fall. These temperature differences are mainly confined to the near-surface and occasionally penetrate throughout the entire water column.

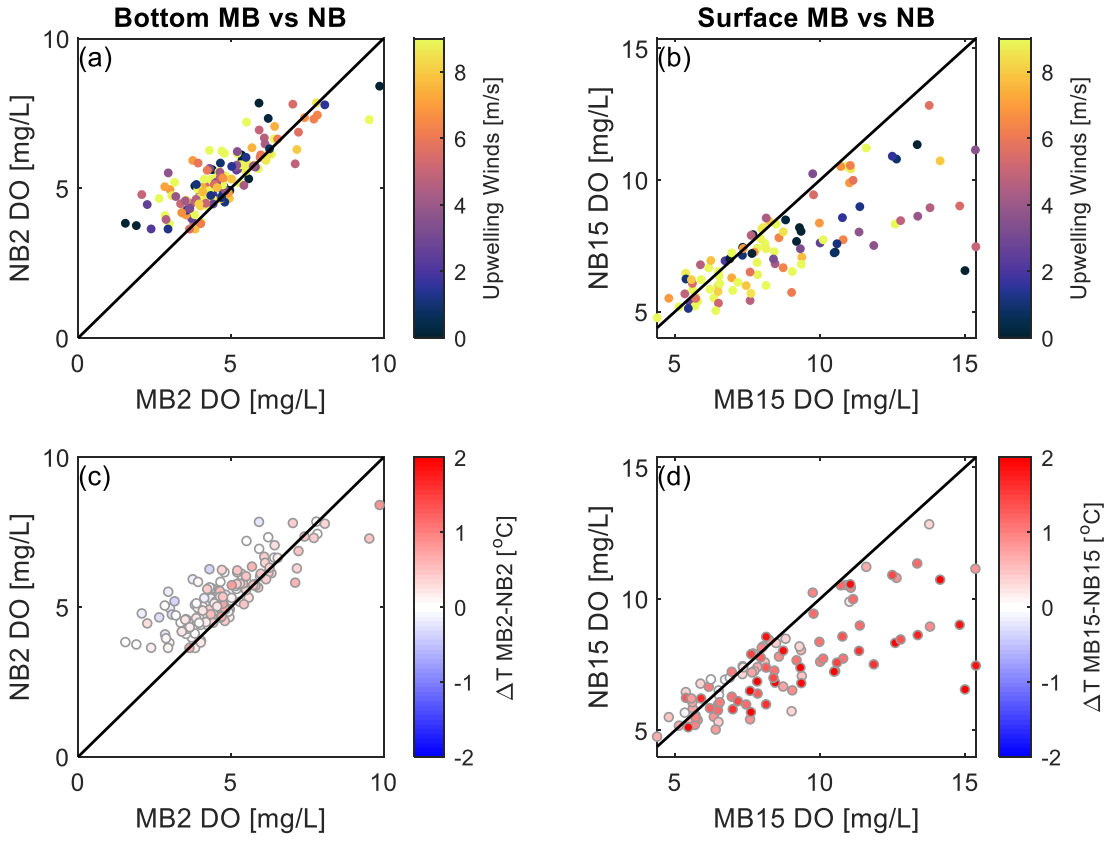

Figure 9: Same as Figure 8, but for MB and NB.

To better characterize the role of phytoplankton community composition on nearshore hypoxia development we compared the relative abundances of diatoms and dinoflagellates taken weekly during the experiment (Figure 11). Diatoms dominated in the low T-DO regime where

near-bottom nearshore T-DO data aligned with the offshore T-DO data, including when the near-bottom data dropped below the hypoxic threshold. Near the surface, diatoms also dominated when the nearshore DO significantly exceeded the offshore T-DO relationship in the high T-DO region. On the other hand, dinoflagellates dominated at the highest temperatures and corresponded to the periods when near-bottom nearshore DO dropped below the offshore T-DO data and the hypoxic threshold range.

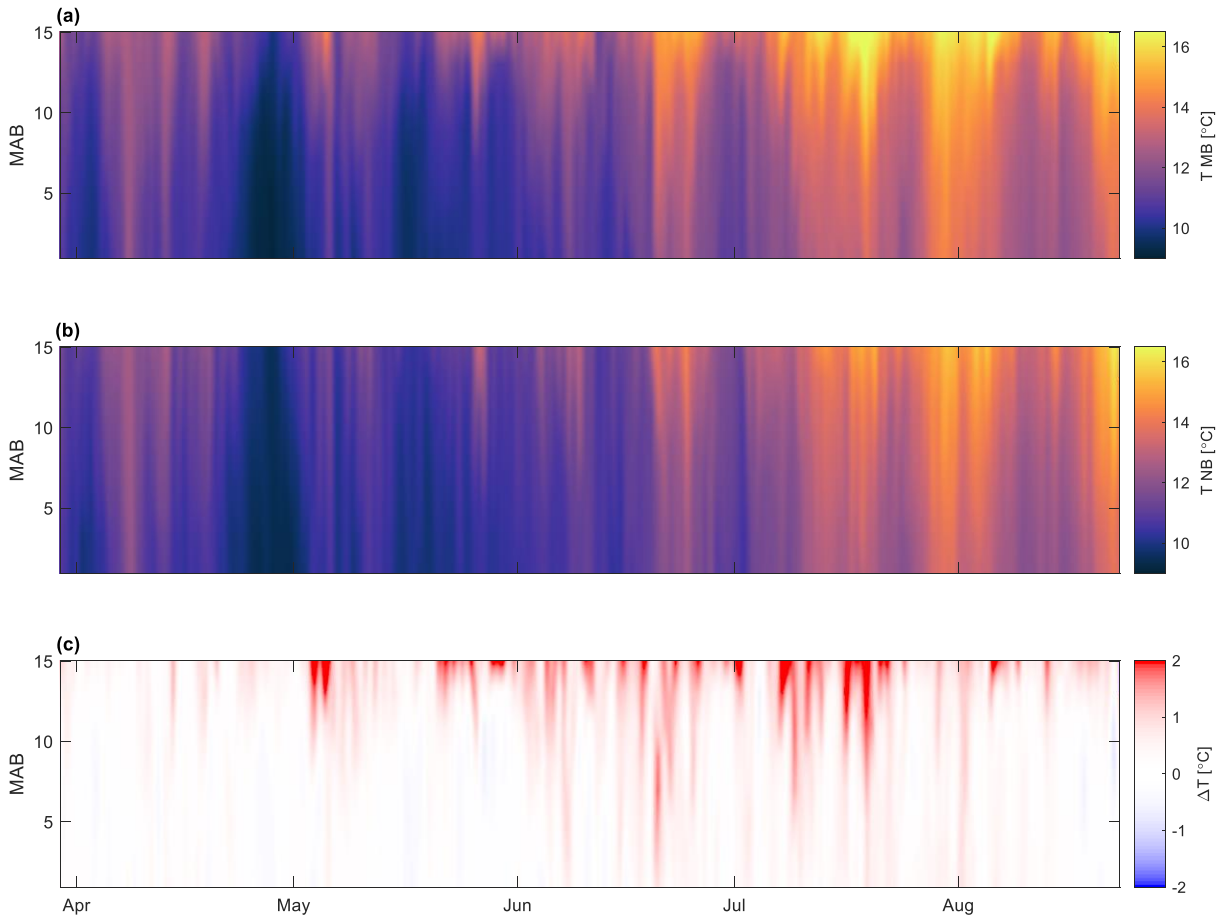

Figure 10: Temperature contour plots over depth and time at (a) MB and (b) NB. (c) Temperature difference between MB and NB. Data are hourly low-passed filtered data.

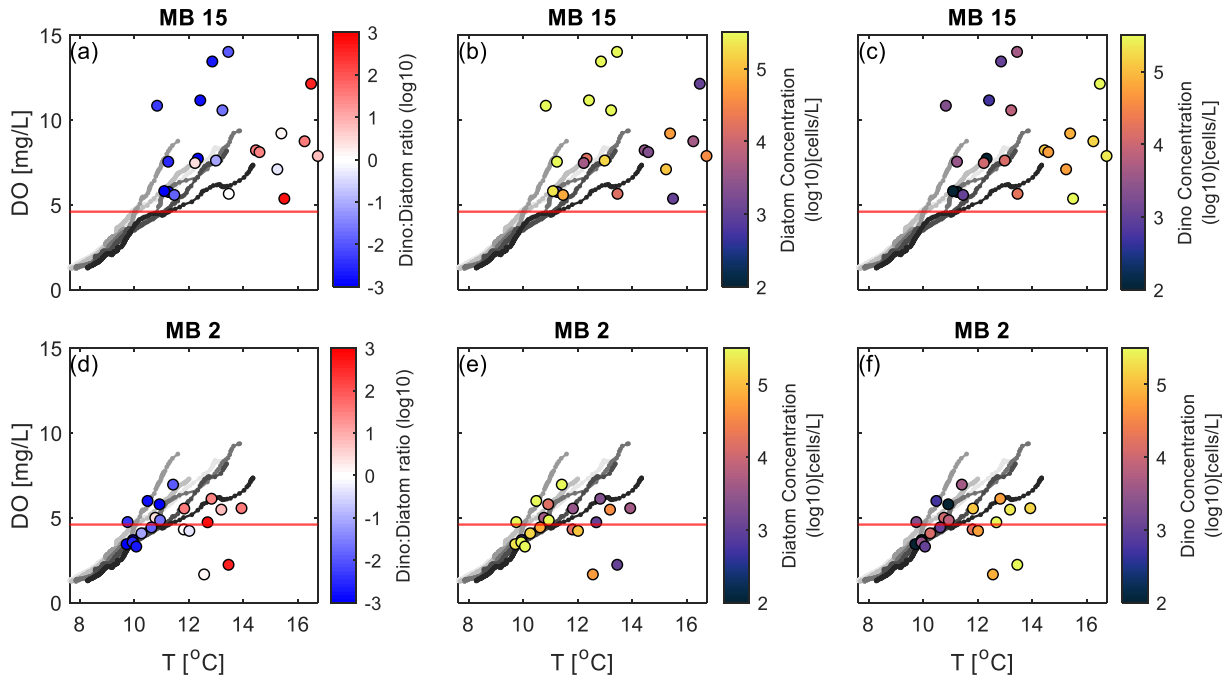

Figure 11: MB surface (a-c) and bottom (d-f) temperature vs DO relationships. Hourly data are low-pass filtered and then downsampled (one point every week) for visualization. Plots (a) and (d) are colored by the log10 of the dinoflagellate:diatom ratio. Plots (b) and (e) are colored by the log10 of diatom concentration. Plots (c) and (f) are colored by the log10 of dinoflagellate concentration. Also shown in each plot in small grayscale points are the offshore T-DO relationship from 300 m, with the earliest cruise in the lightest gray and the latest cruise in black. The hypoxic threshold of 4.6 mg/L is shown as a horizontal red line in all plots.

4 Discussion

4.1 Seasonal Controls

During the late spring and early summer, we found that the nearshore near-bottom T-DO relationship aligned with the deep offshore data during periods of strong upwelling winds, suggesting that the nearshore low DO waters, many of which fell below the hypoxic threshold, were driven by the direct advection of low DO subthermocline waters. This period also coincided with minimal water-column stratification and vertical DO differences in the nearshore, with phytoplankton counts dominated by fast-growing diatoms that thrive in nutrient-rich waters (Silva et al. 2009). These results were consistent across all sites at the near-bottom. In contrast, during the late summer and early fall, the near-bottom nearshore T-DO relationship deviated

significantly from the offshore T-DO relationship, with nearshore DO values much lower than the offshore values for a given temperature. During these deviations, where DO also dropped below the hypoxic threshold, upwelling winds were weak to moderate, and there was significant vertical temperature stratification and vertical DO differences between the top and bottom of the water column. This period was dominated by dinoflagellates, which tend to outcompete diatoms in nutrient-limited and strongly stratified waters (Silva et al. 2009). Given this, the low DO near-bottom nearshore events during the summer and fall are likely driven by the decay of organic matter in the bottom layer and the strong vertical stratification acting as a barrier to vertical mixing and aeration by surface waters. These respiration-driven hypoxic events were observed inside the bay (MB and SB), but not outside the bay (NB), which had significantly fewer hypoxic instances. To further delineate these nearshore hypoxic regimes, we performed a k-means cluster on the nearshore near-bottom data using three clusters and quantified statistics on the environmental conditions in these clusters (Figure 12 and Table 1).

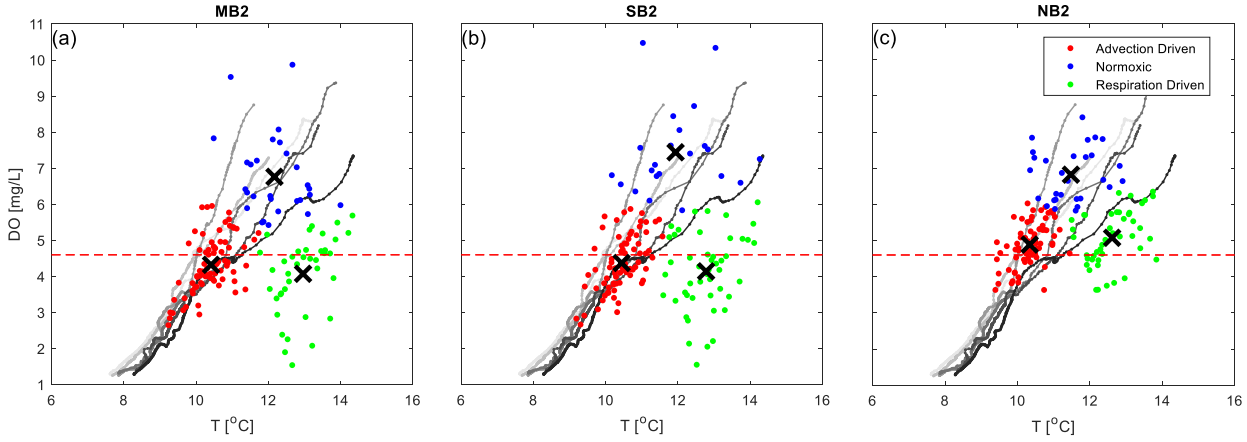

Figure 12: Near-bottom (2 mab) temperature-DO relationship from (a) MB, (b) SB, and (c) NB. Hourly data are low-pass filtered and then downsampled (one point every 24 hrs) for visualization. Colors denote clusters identified by a kmeans cluster analysis, with the black 'X' representing the centroid of the respective cluster. Also shown in each plot in small grayscale points are the offshore T-DO relationship from 300 m, with the earliest cruise in the lightest gray and the latest cruise in black. The hypoxic threshold of 4.6 mg/L is shown as a horizontal red line in all plots.

Table 1: Mean and standard deviation for each of the different clusters at each location. *Data calculated on weekly values unlike the other data columns calculated using daily values.

	Cluster	DO [mg/L]	T [°C]	ΔDO [mg/L]	ΔT [°C]	Upwelling Winds [m/s]	Dino:Diatom Ratio [log10]*
	Advection Driven	4.32 ± 0.77	10.42 ± 0.54	4.02 ± 2.39	1.82 ± 0.63	5.89 ± 4.49	-2.66 ± 1.32
	Normoxic	6.76 ± 1.12	12.17 ± 0.78	3.04 ± 1.53	2.19 ± 0.68	5.99 ± 3.50	-1.02 ± 2.20
MB2	Respiration Driven	4.08 ± 1.07	12.96 ± 0.66	3.67 ± 2.16	2.60 ± 0.57	4.72 ± 2.94	1.10 ± 1.24
	Advection Driven	4.38 ± 0.77	10.44 ± 0.52	4.16 ± 2.15	1.93 ± 0.74	6.01 ± 4.51	-1.73 ± 1.76
	Normoxic	7.44 ± 1.19	11.94 ± 1.06	3.21 ± 1.95	1.66 ± 0.78	5.38 ± 4.06	-2.78 ± 1
SB2	Respiration Driven	4.14 ± 1.06	12.78 ± 0.68	5.01 ± 1.75	2.54 ± 0.54	4.83 ± 2.91	1.31 ± 1.02
	Advection Driven	4.89 ± 0.59	10.34 ± 0.44	2.06 ± 1.20	0.91 ± 0.45	6.07 ± 4.00	-2 ± 1.73
	Normoxic	6.82 ± 0.72	11.48 ± 0.74	2.10 ± 1.63	1.14 ± 0.56	5.82 ± 5.09	-1.82 ± 2.12
NB2	Respiration Driven	5.08 ± 0.75	12.62 ± 0.64	1.63 ± 0.20	1.62 ± 0.32	4.69 ± 2.88	1.29 ± 1.16

4.2 Comparisons to Other Locations

The mechanisms of DO variability observed here have been documented in other coastal environments and embayments. Previous studies done along the California Current System (CCS; Washington State and Central-Oregon continental shelf) have found that upwelling brings low-DO source water into the nearshore; however, source water and near-bottom shelf water with corresponding physical properties were above the hypoxic threshold, highlighting the importance of microbial respiration in the development of hypoxia (Connolly et al. 2010; Adams et al. 2013). In our study, we observed evidence that during strong upwelling events in the spring and early summer, the cross-shelf advection of waters below the hypoxic threshold from the adjacent shelf caused nearshore hypoxia (Figure 6). Additionally, within the greater St. Helena Bay region, along the South African coast, several studies have characterized influences on hypoxia (Baily 1991; Pitcher and Probyn, 2011; Pitcher et al. 2014). Bailey (1991) attributed seasonal near-bottom hypoxia during the late summer and early fall to the decomposition of dinoflagellate blooms and simultaneous stratification. In the same region, Pitcher and Probyn

(2011) observed episodic anoxia throughout the water column during downwelling and unstratified conditions, attributing the signal to the decomposition of organic matter in the source waters during those events. Pitcher (2014) found that both seasonal and episodic hypoxia were largely determined by the role that coastal upwelling plays in controlling bay productivity, and the development, and subsequent decomposition, of phytoplankton blooms. In our study, the lowest DO values observed during the entire experiment coincided with weak to moderate upwelling (i.e., not during downwelling) and strong stratification (Figure 6 and 7), although there were strong differences inside and outside the bay. The observed transition between advection-driven and respiration-driven hypoxia at this location also underpins the importance of intraseasonal upwelling variability (i.e., a seasonal description beyond the common bimodal upwelling and non-upwelling framework, cf. Walter et al. 2018). Moreover, in Southern California, Frieder et al. (2012) found that along-shore gradients in DO near a giant kelp forest (*Macrocystis pyrifera*) were minimal. This directly contrasts our findings that along-shore gradients (e.g., MB vs. NB) were substantial (Figure 9), owing to the role of the upwelling bay on modulating local dynamics and environmental conditions. These results highlight that while many mechanisms are generalizable across study sites and systems, local dynamics and coastline features are critical for assessing hypoxia risk.

4.3 Upwelling Shadow Microclimate

Variation in nearshore responses to physical and biological processes can create marine microclimates that differ from the surrounding region, and in some cases, these can act as marine refuges from the impacts of broader-scale climatic fluctuations (Woodson et al. 2019). Within coastal embayments, reduced wind-driven upwelling creates an upwelling shadow microclimate characterized by anomalously high surface temperatures, a stratified water column, and long

residence times relative to outside the embayment (Graham & Largier, 1997). These conditions make these systems favorable for dinoflagellate blooms, including many HAB species, and as such, they have been termed “bloom incubators” (Ryan et al. 2008). The decomposition of these blooms, and coincident stratification that reduces vertical mixing, can drive hypoxia in the bottom layer (Baily, 1991; Pitcher et al. 2014). We observed this respiration-driven hypoxia inside the SLO Bay upwelling shadow (MB and SB). However, outside of the bay (NB), hypoxic events were largely absent during the same period, with colder temperatures and minimal stratification observed. It is likely that the lack of strong biological respiration, as well as minimally stratified waters, led to conditions favorable for normoxic conditions. These results highlight the important role that coastal embayments and upwelling shadow systems likely play in both local and regional hypoxia development.

4.4 Effects of Climate Change

Low-frequency climate variability [e.g., Pacific Decadal Oscillation (PDO) and North Pacific Gyre Oscillation (NPGO)] and climate change are expected to influence phytoplankton community structure, upwelling seasonality, and intensity, and in turn, nearshore hypoxia. Within, SLO Bay, transitions between different phases of PDO/NPGO coincide with changes in the relative proportion of dinoflagellates and diatoms. In SLO Bay, the positive phase of the PDO (characterized by increased surface temperatures and stratification), dinoflagellate blooms appeared more consistently in the fall and earlier in the seasonal cycle than the negative phase (Barth et al. 2020). The environmental conditions experienced along the California Coast during a positive phase of the PDO are similar to those expected with anthropogenic climate change. It remains to be seen how these shifts in phytoplankton community structure will alter the magnitude and seasonal timing of respiration-driven hypoxia. Additionally, it has been

hypothesized that climate change will enhance upwelling favorable wind stress along EBUS (Bakun 1990). Moreover, several studies found that the upwelling season in EBUS is expected to commence earlier in the year and persist longer into the fall and that this upwelling will advect denser and lower DO source water less frequently, more intensely, and for longer durations, leading to more severe hypoxic events (Iles et al. 2011; Wang et al. 2015; Adams et al. 2013). Within the CCS and the open ocean, climate change-induced ocean warming and increased surface stratification are predicted to lead to further deoxygenation of the world's oceans (Xiu et al. 2018; Mahaffey et al. 2020).

4.5 Future Work

To better illustrate the mechanisms and seasonality of hypoxia in coastal embayments, it is essential to understand the variability from higher frequency processes and phytoplankton structure. Previous studies have shown that high-frequency processes (e.g., internal waves and bores) influence the transport of low-DO water into nearshore habitats (Booth et al. 2012; Walter et al. 2014). In SLO Bay, local diurnal wind forcing has also been known to have a strong influence on temperature variability, occasionally causing intrusions of cold water into the bay, reminiscent of small-scale upwelling (Walter et al. 2017). By further investigating the effect of local diurnal winds and their interaction with other high-frequency processes, we can better assess their influences on nearshore hypoxia development. Additionally, since this study only observed chlorophyll data from inside the bay (MB), future studies should investigate phytoplankton abundance and composition outside the bay. Furthermore, future work should assess the role that phytoplankton community structure (e.g., diatoms versus dinoflagellates), and the subsequent decomposition, play in controlling nearshore DO variability (Spilling et al. 2018).

5 Conclusion

Dissolved oxygen (DO) is an important biogeochemical factor that strongly influences nearshore coastal ecosystems. Low DO (hypoxic) events can cause physiological stressful environments for ecological and economically important species, potentially leading to mass mortalities. In order to better assess drivers of coastal hypoxia, we collected data from monthly cruises on the inner shelf and nearshore moorings inside and outside a small coastal embayment (San Luis Obispo Bay on the Central California Coast) across the full upwelling season (March to August). During the late spring and early summer, we found that the nearshore near-bottom temperature-DO (T-DO) relationship aligned with the shelf data during periods of strong upwelling winds, suggesting that the nearshore low DO waters, many of which fell below the hypoxic threshold, were driven by the direct advection of low DO subthermocline waters. This period also coincided with minimal water-column stratification and vertical DO differences across all sites in the nearshore, with phytoplankton counts dominated by diatoms. In contrast, during the late summer and early fall, the near-bottom nearshore T-DO relationship deviated significantly from the offshore T-DO relationship, with nearshore DO values much lower than those offshore for a given temperature. During these deviations, where DO also dropped below the hypoxic threshold, upwelling winds were weak to moderate, there was significant vertical temperature stratification and vertical DO differences, and phytoplankton counts were dominated by dinoflagellates. These near-bottom hypoxic events were likely driven by the decay of organic matter in the bottom layer and the strong stratification that prevented vertical mixing. These respiration-driven events were observed inside the bay, but not outside the bay, highlighting the role of the coastal embayment and this upwelling shadow system on local hypoxia development. The seasonal transition between advection-driven and respiration-driven hypoxia in the CCS is a

novel finding, with important implications for assessing nearshore hypoxia risk in a changing climate. While tuned specifically for SLO Bay, these findings can be used as a baseline for similar upwelling embayments.

6 Acknowledgements

This work was supported by California Sea Grant (Award NA14OAR417007). We acknowledge support from the NOAA IOOS program through CeNCOOS (Shore Stations) and SCCOOS (HABs) for data collected at the Cal Poly Pier. We also acknowledge support from The William and Linda Frost Fund. I would like to thank Ian Robbins and Dr. Alexis Pasulka for providing valuable resources and their expertise in their field of work. Most importantly, thank you to Dr. Ryan Walter for providing me with this opportunity as well as guidance and encouragement throughout this project and my academic career. The knowledge and skills, he has bestowed with me will be invaluable in my future ambitions.

References

Adams, K. A., Barth, J. A., & Chan, F. (2013). Temporal variability of near-bottom dissolved oxygen during upwelling off central Oregon. *Journal of Geophysical Research: Oceans*, *118*(10), 4839-4854. https://doi.org/10.1002/jgrc.20361

Bailey, G. W. (1991). Organic carbon flux and development of oxygen deficiency on the modern Benguela continental shelf south of 22 S: spatial and temporal variability. *Geological Society, London, Special Publications*, *58*(1), 171-183. https://doi.org/10.1144/GSL.SP.1991.058.01.12

Bakun, A. (1990). Global climate change and intensification of coastal ocean upwelling. *Science*, *247*(4939), 198-201. 10.1126/science.247.4939.198

Barth, A., Walter, R. K., Robbins, I., & Pasulka, A. (2020). Seasonal and interannual variability of phytoplankton abundance and community composition on the Central Coast of California. *Marine Ecology Progress Series*, *637*, 29-43. https://doi.org/10.3354/meps13245

Boehm, A. B., Jacobson, M. Z., O'Donnell, M. J., Sutula, M., Wakefield, W. W., Weisberg, S. B., & Whiteman, E. (2015). Ocean acidification science needs for natural resource managers of the North American west coast. *Oceanography*, *28*(2), 170-181. https://www.jstor.org/stable/24861879

Booth, J.A.T., McPhee-Shaw, E.E., Chua, P., Kingsley, E., Denny, M., Phillips, R., Bograd, S.J., Zeidberg, L.D. and Gilly, W.F. (2012). Natural intrusions of hypoxic, low pH water into nearshore marine environments on the California coast. *Continental Shelf Research*, *45*, 108-115. https://doi.org/10.1016/j.csr.2012.06.009

Chan, F., Barth, J. A., Lubchenco, J., Kirincich, A., Weeks, H., Peterson, W. T., & Menge, B. A. (2008). Emergence of anoxia in the California current large marine ecosystem. *Science*, *319*(5865), 920-920. 10.1126/science.1149016

Chavez, F. P., & Messié, M. (2009). A comparison of eastern boundary upwelling ecosystems. *Progress in Oceanography*, *83*(1-4), 80-96. https://doi.org/10.1016/j.pocean.2009.07.032

Connolly, T. P., Hickey, B. M., Geier, S. L., & Cochlan, W. P. (2010). Processes influencing seasonal hypoxia in the northern California Current System. *Journal of Geophysical Research: Oceans*, *115*(C3). https://doi.org/10.1029/2009JC005283

Du, J., Shen, J., Park, K., Wang, Y. P., & Yu, X. (2018). Worsened physical condition due to climate change contributes to the increasing hypoxia in Chesapeake Bay. *Science of the Total Environment*, *630*, 707-717. 10.1016/j.scitotenv.2018.02.265

Frieder, C. A., Nam, S. H., Martz, T. R., & Levin, L. A. (2012). High temporal and spatial variability of dissolved oxygen and pH in a nearshore California kelp forest. *Biogeosciences*, *9*(10), 3917-3930. https://doi.org/10.5194/bg-9-3917-2012

García-Reyes, M., & Largier, J. L. (2012). Seasonality of coastal upwelling off central and northern California: New insights, including temporal and spatial variability. *Journal of Geophysical Research: Oceans*, *117*(C3). https://doi.org/10.1029/2011JC007629

Graham, W. M., & Largier, J. L. (1997). Upwelling shadows as nearshore retention sites: the example of northern Monterey Bay. *Continental Shelf Research*, *17*(5), 509-532. https://doi.org/10.1016/S0278-4343(96)00045-3

Grantham, B.A., Chan, F., Nielsen, K.J., Fox, D.S., Barth, J.A., Huyer, A., Lubchenco, J. and Menge, B.A. (2004). Upwelling-driven nearshore hypoxia signals ecosystem and oceanographic changes in the northeast Pacific. *Nature*, *429*(6993), 749-754. https://doi.org/10.1038/nature02605

Iles, A. C., Gouhier, T. C., Menge, B. A., Stewart, J. S., Haupt, A. J., & Lynch, M. C. (2012). Climate-driven trends and ecological implications of event-scale upwelling in the California Current System. *Global Change Biology*, *18*(2), 783-796. https://doi.org/10.1111/j.1365-2486.2011.02567.x

Largier, J. L. (2020). Upwelling bays: how coastal upwelling controls circulation, habitat, and productivity in bays. *Annual review of marine science*, *12*, 415-447. https://doi.org/10.1146/annurev-marine-010419-011020

Mahaffey, C., Palmer, M., Greenwood, N., & Sharples, J. (2020). Impacts of climate change on dissolved oxygen concentration relevant to the coastal and marine environment around the UK. *MCCIP Science Review*, *2002*, 31-53. https://doi.org/10.14465/2020.arc02.oxy

Pennington, J. T., & Chavez, F. P. (2000). Seasonal fluctuations of temperature, salinity, nitrate, chlorophyll and primary production at station H3/M1 over 1989–1996 in Monterey Bay, California. *Deep Sea Research Part II: Topical Studies in Oceanography*, *47*(5-6), 947-973. https://doi.org/10.1016/S0967-0645(99)00132-0

Pitcher, G. C., & Probyn, T. A. (2011). Anoxia in southern Benguela during the autumn of 2009 and its linkage to a bloom of the dinoflagellate Ceratium balechii. *Harmful Algae*, *11*, 23-32. https://doi.org/10.1016/j.hal.2011.07.001

Pitcher, G.C., Probyn, T.A., du Randt, A., Lucas, A.J., Bernard, S., Evers-King, H., Lamont, T. and Hutchings, L. (2014). Dynamics of oxygen depletion in the nearshore of a coastal embayment of the southern Benguela upwelling system. *Journal of Geophysical Research: Oceans*, *119*(4), 2183-2200. https://doi.org/10.1002/2013JC009443

Ryan, J.P., Gower, J.F., King, S.A., Bissett, W.P., Fischer, A.M., Kudela, R.M., Kolber, Z., Mazzillo, F., Rienecker, E.V. and Chavez, F.P. (2008). A coastal ocean extreme bloom incubator. *Geophysical Research Letters*, *35*(12). https://doi.org/10.1029/2008GL034081

Silva, A., Palma, S., Oliveira, P. B., & Moita, M. T. (2009). Composition and interannual variability of phytoplankton in a coastal upwelling region (Lisbon Bay, Portugal). *Journal of Sea Research*, *62*(4), 238-249. https://doi.org/10.1016/j.seares.2009.05.001

Spilling, K., Olli, K., Lehtoranta, J., Kremp, A., Tedesco, L., Tamelander, T., Klais, R., Peltonen, H. and Tamminen, T. (2018). Shifting diatom—dinoflagellate dominance during spring bloom in the Baltic Sea and its potential effects on biogeochemical cycling. *Frontiers in Marine Science*, *5*, 327. https://doi.org/10.3389/fmars.2018.00327

Vaquer-Sunyer, R., & Duarte, C. M. (2008). Thresholds of hypoxia for marine biodiversity. *Proceedings of the National Academy of Sciences*, *105*(40), 15452-15457. https://doi.org/10.1073/pnas.0803833105

Walter, R. K., Armenta, K. J., Shearer, B., Robbins, I., & Steinbeck, J. (2018). Coastal upwelling seasonality and variability of temperature and chlorophyll in a small coastal embayment. *Continental Shelf Research*, *154*, 9-18. https://doi.org/10.1016/j.csr.2018.01.002

Walter, R. K., Reid, E. C., Davis, K. A., Armenta, K. J., Merhoff, K., & Nidzieko, N. J. (2017). Local diurnal wind-driven variability and upwelling in a small coastal embayment. *Journal of Geophysical Research: Oceans*, *122*(2), 955-972. https://doi.org/10.1002/2016JC012466

Walter, R. K., Woodson, C. B., Leary, P. R., and Monismith, S. G. (2014), Connecting wind-driven upwelling and offshore stratification to nearshore internal bores and oxygen variability, *J. Geophys. Res. Oceans*, 119, 3517– 3534, https://doi.org/10.1002/2014JC009998

Wang, D., Gouhier, T. C., Menge, B. A., & Ganguly, A. R. (2015). Intensification and spatial homogenization of coastal upwelling under climate change. *Nature*, *518*(7539), 390-394. https://doi.org/10.1038/nature14235

Woodson, C.B., Micheli, F., Boch, C., Al-Najjar, M., Espinoza, A., Hernandez, A., Vázquez-Vera, L., Saenz-Arroyo, A., Monismith, S.G. and Torre, J. (2019). Harnessing marine microclimates for climate change adaptation and marine conservation. *Conservation Letters*, *12*(2), e12609. https://doi.org/10.1111/conl.12609

Woodson, C.B., Washburn, L., Barth, J.A., Hoover, D.J., Kirincich, A.R., McManus, M.A., Ryan, J.P. and Tyburczy, J. (2009). Northern Monterey Bay upwelling shadow front: Observations of a coastally and surface-trapped buoyant plume. *Journal of Geophysical Research: Oceans*, *114*(C12). https://doi.org/10.1029/2009JC005623

Xiu, P., Chai, F., Curchitser, E. N., & Castruccio, F. S. (2018). Future changes in coastal upwelling ecosystems with global warming: The case of the California Current System. *Scientific reports*, *8*(1), 1-9. https://doi.org/10.1038/s41598-018-21247-7